Bomb-radiocarbon signal suggests that soil carbon contributes to chlorophyll *a* in archival oak leaves

Naoto F. Ishikawa[1, 2], Hisami Suga[1], Tessa S. van der Voort[2], Reto Nyffeler[3], Nanako O. Ogawa[1], Negar Haghipour[2, 4], Lukas Wacker[4], Timothy I. Eglinton[2] and, Naohiko Ohkouchi[1]

[1]Japan Agency for Marine-Earth Science and Technology, Yokosuka 237-0061, Japan
[2]Department of Earth Sciences, ETH Zürich, 8092 Zürich, Switzerland
[3]Department of Systematic and Evolutionary Botany, University of Zürich, 8008 Zürich, Switzerland
[4]Laboratory for Ion Beam Physics, ETH Zürich, 8093 Zürich, Switzerland

Correspondence to: Naoto F. Ishikawa (ishikawan@jamstec.go.jp)

Abstract. Carbon exchange between biosphere and rhizosphere is an important component of the global carbon cycle. Photosynthetic products being sequestered into soils have been intensively studied, yet the reverse pathway from rhizosphere to biosphere is poorly known. In the present study, we determined the radiocarbon content ($\Delta^{14}C$) of the bulk leaves of the deciduous *Quercus* oak and of chlorophyll *a* extracted from the same leaves collected in Switzerland during the 1950s and 2000s. Our results demonstrate that old soil-derived carbon significantly contributes to the synthesis of chlorophyll *a*, an essential molecule for photoautotrophs. The $\Delta^{14}C$ values of chlorophyll *a* were consistently lower than those of bulk leaves which closely tracked bomb-derived $\Delta^{14}C$ signals in the atmosphere. The results cannot be explained without invoking an additional carbon source with a turnover time exceeding 100 years. A two-pool mixing model assuming atmosphere and rhizosphere as two endmembers indicates that contributions of the soil carbon to chlorophyll *a* are 17 ± 2% (n = 4), and turnover time of such soil carbon is no shorter than 1,000 years. We suggest that hydrophilic compounds such as amino acids or phytol are transferred into plant roots from soils through mycorrhizal symbionts, and chlorophyll *a* is one of the destinations of such ^{14}C-depleted carbon in vascular plants.

1 Introduction

Terrestrial vegetations play a pivotal role in global carbon cycle by converting atmospheric CO_2 into organic matter via photosynthesis. A large portion of photosynthesized products is then sequestered into rhizosphere as soil organic matter over centennial or millennial time scale (Clemmensen et al., 2013). In a microscopic spatial scale, most of terrestrial vascular plants accommodate mycorrhizal fungi on their roots, where plants give carbon to fungi while fungi return nutrients and water to plants (Smith and Read, 2008). Conventional theory predicts such a one-directional carbon flow, however, there is a growing body of evidence suggesting that some ectomycorrhizal trees gain even carbon from symbiotic fungi, most likely as inorganic forms such as HCO_3^- or hydrophilic compounds such as amino acids available in rhizosphere (Jones et al., 2009). Previous studies have primarily focused on quantifying carbon flow between fungi and plants, exploring functional diversity in the

symbiosis, or unraveling plant-mycorrhiza-plant communications (Cahanovitc et al., 2022; Klein et al., 2016; Simard et al., 1997; Suetsugu et al., 2020). However, one grand challenge, why and how plants uptake the soil carbon that have been unconsidered as a limiting element for their growth, remains unsolved. Fate or destination of such soil carbon in plants is particularly unknown, which hinders from drawing the entire picture of carbon exchange between biosphere and rhizosphere. It is expected that the soil carbon offers some benefit to plants. Their growth is more limited by nitrogen, which is mainly acquired as water-soluble inorganic forms such as nitrate and ammonium via root uptake and xylem translocation, although plants are still deficient in nitrogen, eventually resulting in yellowed leaves called chlorosis (Taiz et al., 2023). To tackle this issue, the plant may also uptake organic nitrogen such as amino acids from soil (Näsholm et al., 1998) as a building block for some functional compounds that cost energy to synthesize. Chlorophyll *a* (Chl *a*, $C_{55}H_{72}MgN_4O_5$, molecular weight 893.51 g mol^{-1}) is one of the candidate compounds, which is an antenna pigment ubiquitous for a variety of photosynthetic autotrophs, including terrestrial plants, aquatic algae, and cyanobacteria, to convert solar energy to chemical energy. The Chl *a* consists of a tetrapyrrole ring, which is synthesized from glutamic acid, and its side chain, phytol, which is added at the very end of its anabolism catalyzed by a single enzyme named chlorophyll synthase (von Wettstein et al., 1995). In contrast, phytol is removed from Chl *a* by pheophytinase at one of the very first reactions of its catabolism, followed by a sequence of break-down reactions of the tetrapyrrole ring (Matile et al., 1999). Due to the high maintenance cost, some vascular plants and microalgae have a recycling pathway in the Chl *a* metabolism (Ischebeck et al., 2006; Vavilin and Vermaas, 2007), suggesting that its 55 carbon atoms are potentially derived from multiple sources. To test the hypothesis that carbon originated from rhizosphere is partially used for Chl *a* biosynthesis, it is necessary to distinguish soil-derived carbon from annual photosynthates.

Radiocarbon natural abundance ($\Delta^{14}C$) offers a unique opportunity to address the above question. The atmospheric hydrogen-bomb tests mainly during the late 1950s and early 1960s almost doubled $^{14}CO_2$ concentrations (i.e., the $\Delta^{14}C$ value for CO_2 increased by ~+1000‰) in the Northern Hemisphere atmosphere (Nydal and Lövseth, 1965). Since the Partial Test Ban Treaty (PTBT) took effect in 1963 CE, the atmospheric $^{14}CO_2$ concentration has declined continuously due to dissolution into the ocean and biosphere as well as dilution by fossil-fuel combustion (Levin and Kromer, 2004). On the other hand, atmospheric $^{14}CO_2$ is fixed by terrestrial plants and is reflected in $\Delta^{14}C$ of annually growing plant tissues such as tree ring (Hua et al., 2004). Annual leaves of deciduous plants are also a good recorder of atmospheric $^{14}CO_2$ concentrations because they consist of 1–2-year-old carbon on average (Ichie et al., 2013; Muhr et al., 2016). Taking advantage of this, previous studies have estimated carbon residence time of different components within a plant (Carbone et al., 2013; Richardson et al., 2015), as well as belowground root and soil interactions (Gaudinski et al., 2000; Trumbore, 2000).

To estimate their age, compound-specific radiocarbon analysis (CSRA) of Chl *a* and its derivatives was first applied to sediments in Black Sea (Kusch et al., 2010). They found a large variation by nearly 200‰ in $\Delta^{14}C$ among different pigments in the same station. A similar size of $\Delta^{14}C$ variation was also found in pigments and fatty acids in a lake near Mount Fuji (Yamamoto et al., 2020). To our knowledge, these two studies are the only examples that used the CSRA of Chl *a* and other pigments in sediments. Furthermore, our previous study indicated that the $\Delta^{14}C$ value of Chl *a* (–10‰) in a leaf of the Japanese blue oak, *Quercus glauca*, was lower than that of its bulk $\Delta^{14}C$ value (+27‰). Although the results suggest that *Q. glauca*

Deleted: terrestrial

Deleted: cycle

synthesize Chl *a* partially using carbon likely derived from rhizosphere, this is not conclusive yet because the difference in $\Delta^{14}C$ values between the bulk leaf and its Chl *a* (37‰) was not sufficiently large compared to the analytical error with no replicate data.

In this study, we aimed to test whether the $\Delta^{14}C$ values of the bulk leaf and its Chl *a* are significantly different in terrestrial vascular plants using eight *Quercus* leaf samples that had been collected during 1952 and 2007 CE. A retrospective analysis during the post-PTBT (i.e., after 1963) period was expected to distinguish atmospheric CO_2 being highly enriched in ^{14}C compared to soil carbon. The genus *Quercus* is one of the ectomycorrhizal trees that is known to exchange carbon through the root-fungal network (Klein et al., 2016; Simard et al., 1997) whose genus is the same with that reported in our previous study (Ishikawa et al., 2015). We isolated and purified Chl *a* from archival leaves using high performance liquid chromatography to measure its $\Delta^{14}C$ value in comparison with the bulk leaf. We hypothesized that the $\Delta^{14}C$ value of the bulk leaf reflect that of atmospheric CO_2 at the time of collection, while the $\Delta^{14}C$ value of Chl *a* is different from that of the bulk, due to the contribution from soil carbon that has turnover time longer than annual photosynthetic products. We built a two-pool model to specifically address two research questions: (1) how many percentages of soil carbon is incorporated into Chl *a*; and (2) how old is soil carbon contributing to the Chl *a*.

2 Materials and methods

2.1 Sample collection

Two species of deciduous *Quercus* oak (Downy oak *Quercus pubescens* and Sessile oak *Quercus petraea*) that had been collected in Switzerland during 1952 and 2007 and have been stored in the University of Zürich Herbarium (n = 8) under constant temperature and humidity conditions were dedicated to the retrospective analysis of this study (Fig. 1a). One leaf of the bunch was sampled for *Q. pubescens*, n = 5, collected on 11 August 1952 (converted to decimal year: 1952.611, leap year), 15 August 1965 (1965.622), 14 September 1968 (1968.704, leap year), 3 July 1973 (1973.504), and 2 July 1982 (1982.502); and *Q. petraea*, n = 3, collected on 30 May 1966 (1966.411), 25 May 1995 (1995.398), and 8 July 2007 (2007.518). The specimen labels provided us fragmentary information such as altitude and location where the samples were collected (Table 1). Approximately 3 mg of the leaf samples were cut by clean tweezers for the bulk $\Delta^{14}C$ measurement. Remaining leaf samples were stored at –20 ºC until the following analysis.

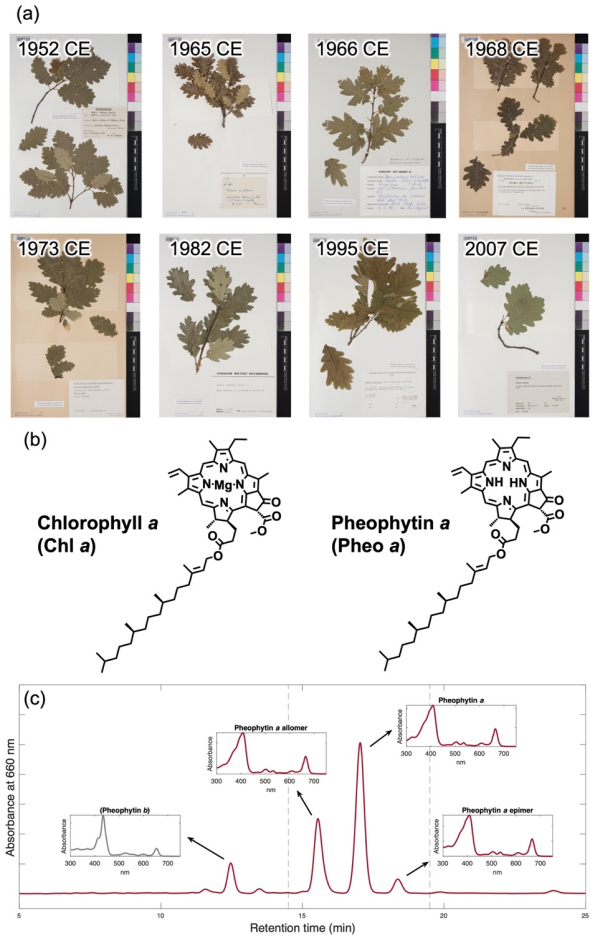

Figure 1: (a) The *Quercus* leaf samples collected in 1952 CE (*Q. pubescens*), 1965 CE (*Q. pubescens*), 1966 CE (*Q. petraea*), 1968 CE (*Q. pubescens*), 1973 CE (*Q. pubescens*), 1982 CE (*Q. pubescens*), 1995 CE (*Q. petraea*), and 2007 CE (*Q. petraea*). One leaf per sample was dedicated for analysis; (b) Chemical structures of Chl *a* and Pheo *a*; and (c) Representative HPLC/DAD chromatograms at 660 nm absorbance of pigments extracted from *Q. pubescens* collected in 1968 CE. The DAD spectrums of the three major peaks are shown in inset figures. Dashed lines indicate start and end times of fraction collections (Pheo *a* and its allomer and epimer) that were combined for radiocarbon analysis. Pheo *b* and its derivatives were not used due to their insufficient amount for CSRA.

Table 1: Summary of dataset analyzed in this study. UZH: University of Zürich; IAA: Institute of Accelerator Analysis; CSRA: Compound-Specific Radiocarbon Analysis; MICADAS: MIniature CArbon DAting System

Reference code	UZH ZT-00137600	UZH ZT-00137603	UZH ZT-00137619	UZH ZT-00137601	UZH ZT-00137608	UZH ZT-00137607	UZH ZT-00137615	UZH ZT-00137
Species	*Q. pubescens*	*Q. pubescens*	*Q. petraea*	*Q. pubescens*	*Q. pubescens*	*Q. pubescens*	*Q. petraea*	*Q. petraea*
Date collected	1952/08/11	1965/08/15	1966/05/30	1968/09/14	1973/07/03	1982/07/02	1995/05/25	2007/07/08
Description								
Altitude (m)	500	530	520		700		1140	580
Notes		Kanton Zürich				Hügel Ravouire, ca. 1.5 km NE from Sierre, VS		Kanton Zürich, some influence f *Q. pubescens*
Bulk leaf								
$\delta^{13}C$ (‰)	-26.9	-25.3	-26.9	-28.2	-24.1	-26.4	-27.4	-28.2
$\delta^{15}N$ (‰)	-5.7	-0.7	1.4	-4.5	-3.8	-4.8	-3.0	-4.9
C/N	23.0	19.7	17.3	17.9	22.6	17.2	22.9	19.9
$F^{14}C$	0.961	1.761	1.703	1.573	1.444	1.249	1.105	1.053
error	0.003	0.004	0.004	0.004	0.004	0.003	0.003	0.003
$\Delta^{14}C$ (‰)	-46.8	746.8	689.0	560.2	431.7	238.6	96.1	44.0
AMS error (1σ, ‰)	±2.6	±4.0	±3.7	±3.6	±3.4	±3.0	±3.0	±2.8
IAA code	IAAA-180297	IAAA-180300	IAAA-180316	IAAA-180298	IAAA-180305	IAAA-180304	IAAA-180312	IAAA-18031
Cal a								
$\delta^{13}C$ (‰)	-28.7	-26.0	-30.1	-28.9	-25.4	-27.0	-28.4	-29.6
$\delta^{15}N$ (‰)	-5.3	2.7	2.4	-3.0	-4.5	-3.1	-5.3	-5.0
C/N	13.6	14.7	16.3	14.0	12.6	12.7	12.3	10.7
µgC for CSRA	40	24	16	40	40	40	40	52
$F^{14}C$	0.928	1.614	1.639	1.509	1.379	1.204	1.066	1.015
error	0.008	0.007	0.008	0.007	0.007	0.008	0.008	0.008
$\Delta^{14}C$ (‰)	-80.3	599.7	624.1	495.1	366.6	192.8	56.4	5.1
MICADAS error (1σ, ‰)	±8.1	±7.1	±7.9	±7.3	±7.3	±7.5	±7.9	±8.1
ETH code	140984.1.1	140978.1.1	140979.1.1	140985.1.1	140987.1.1	140986.1.1	140988.1.1	140983.1.1
Plausible Model								
P_S (%)	29%	13%	11%	20%	19%	15%	18%	15%
T_S (years)	2000	1700	1000	500	1000	2200	2600	2000
$\Delta\Delta^{14}C$ (‰)	0.02	0.03	0.01	<0.01	<0.01	<0.01	0.01	<0.01

Formatted Table ... [1]
Formatted ... [2]
Formatted ... [3]
Formatted ... [4]
Formatted ... [5]
Formatted ... [6]
Formatted ... [7]
Formatted ... [8]
Formatted ... [9]
Formatted ... [10]
Formatted ... [11]
Formatted ... [12]
Formatted ... [13]
Formatted ... [14]
Formatted ... [15]
Formatted ... [16]
Formatted ... [17]
Formatted ... [18]
Formatted ... [19]
Formatted ... [20]
Formatted ... [21]
Formatted ... [22]
Formatted ... [23]
Formatted ... [24]
Formatted ... [25]
Formatted ... [26]
Formatted ... [27]
Formatted ... [28]
Formatted ... [29]
Formatted ... [30]
Formatted ... [31]
Formatted ... [32]
Formatted ... [33]
Formatted ... [34]
Formatted ... [35]
Formatted ... [36]
Formatted ... [37]
Formatted ... [38]
Formatted ... [39]
Formatted ... [40]
Formatted ... [41]
Formatted ... [42]
Formatted ... [43]
Formatted ... [44]
Formatted ... [45]
Formatted ... [46]
Deleted: 28%
Deleted: 13%
Deleted: 10%
Deleted: 15%
Deleted: 17%
Deleted: 13%
Deleted: 18%
Deleted: 26%

2.2 Preparation for chlorophyll *a*

Chl *a* was extracted from each leaf sample using the modified method of Ishikawa et al., (2015) In brief, crude pigments were extracted from 100–200 mg of dried and crushed leaves using about 30 mL of acetone in a PTFE tube (Oak Ridge Centrifugal Tube, 3114-0050, Thermo Scientific, USA). The tubes were ultrasonicated for 15 min and were centrifugated at 4,000 rpm for 30 min. The supernatant was transferred into a pre-combusted glass vial (ASE collection vial 60 mL, 048784, Thermo) and was dried under the argon stream. About 2 mL of dimethylformamide (DMF) was added to the PTFE tube, ultrasonicated, centrifugated, and transferred into the 60 mL glass vial. The DMF extraction was repeated one more time to increase the recovery. After drying up the samples, they were transferred using dichloromethane (DCM) into a pre-combusted glass vial (4 mL screw vial, 5183-4448, Agilent Technologies, USA) and were dried using argon. Since the extracted Chl *a* is quickly degraded at room temperature in laboratory, about 1 mL of 2 mol mL^{-1} hydrochloric acid was added to the vial to convert Chl *a* into pheophytin *a* (Pheo *a*) to increase stability. Therefore, the present study regards Pheo *a* as a surrogate of Chl *a*, and does not consider a potential difference in $\Delta^{14}C$ values between Chl *a* and Pheo *a*. The only difference between Chl *a* and Pheo *a* is the presence or absence of magnesium at the center of the tetrapyrrole ring (Fig. 1b). About 1 mL of *n*-hexane was added to the vial, and the liquid-liquid extraction was made three times, and the organic layer was transferred into another 4 mL vial. After drying up, a 0.2 mL of DMF was added to the vial and the solution was passed through a membrane filter (Cosmospin Filter G, pore size 0.2 µm, 06549-44, Merck, Germany) and recovered in a pre-combusted 1.2 mL glass vial (Supelco 29658-U, Merck).

The acidified crude pigment dissolved in DMF was injected to a high-performance liquid chromatography (HPLC) system (1260 Infinity, Agilent Technologies) for the first separation using a reversed-phase column (Eclipse XDB-C18, 5 µm particle size, 4.6 × 250 mm, P/N 990967-902, Agilent Technologies) with the corresponding guard column (5 µm particle size, 4.6 × 12.5 mm, Agilent Technologies). All the solvent used in the following wet chemical operation was higher than the HPLC grade. The solvent gradient was programmed as follows: acetonitrile: ethyl acetate: pyridine = 75:25:0.5 (v/v/v) held for 5 min, then gradually changed to 67.5:32.5:0.5 (v/v/v) in 15 min, followed by flushing (25:75:0.5, v/v/v for 5 min) and equilibration (75:25:0.5, v/v/v for 5 min). The flow rate and temperature were set constant at 1.0 mL min^{-1} and 30 ºC, respectively. Three injections were made per sample, and Pheo *a* and its allomer and epimer were collected using a fraction collector based on their retention times (14.5–16.0 min, 16.0–18.0 min, and 18.0–19.5 min, respectively) at the 660 nm wavelength of the diode array detector (DAD). The concentration of Pheo *a* and its derivatives (0.2–0.7 µg mg^{-1}) was two orders of magnitude smaller than that typically found in fresh *Quercus* leaves (10–20 µg mg^{-1}, Rodríguez-Calcerrada et al., 2008), probably due to significant amounts of degradation during the long-term storage. However, the degradation does not impact radiocarbon ($\Delta^{14}C$) results because any isotopic fractionation during the storage up to 70 years is internally corrected by $\delta^{13}C$ values (see section 2.5 Radiocarbon measurements). It should also be mentioned that the Chl *a* survived after all is obviously intact because non-photoautotrophs such as fungi potentially colonizing the leaf surface during the storage in the herbarium cannot synthesize Chl *a*. Pheo *b* and its derivatives (allomer and epimer) being also found in the chromatogram

Deleted: 6
Deleted: 8
Deleted: 5
Deleted: 6
Deleted: 5
Formatted: Superscript

(Fig. 1c) were not collected because their concentrations were too small to implement the CSRA measurement. These fractions were combined in a pre-combusted 6 mL glass vials, dried under the argon stream, and re-dissolved in a 0.2 mL of DMF.

The Pheo *a* fraction after the above first separation was re-introduced to the HPLC for the second separation using another column (Eclipse PAH, 5 µm particle size, 4.6 × 250 mm, P/N 959990-918, Agilent Technologies). The solvent gradient was programmed as follows: acetonitrile: ethyl acetate: pyridine = 80:20:0.5 (v/v/v) held for 5 min, then gradually changed to 32:68:0.5 (v/v/v) in 18 min, followed by equilibration (80:20:0.5, v/v/v for 5 min). The flow rate and temperature were set constant at 1.0 mL min^{-1} and 15 ºC, respectively. Three injections were made per sample, and the Pheo *a* was re-collected based on their retention times (16.5–17.8 min for allomer, 17.8–19.2 min for Pheo *a*, and 19.2–20.5 min for epimer) at the 660 nm wavelength. After drying the Pheo *a* fractions, the liquid-liquid extraction was made using water:*n*-hexane:DCM (1:0.7:0.3, v/v) three times and the organic layer was transferred into a pre-combusted 1.2 mL glass vial. The vial was dried using argon and kept at –20 ºC until the following analysis.

Deleted: 3

Deleted: 1

Deleted: using DCM

2.3 Carbon and nitrogen stable isotope measurements

We determined stable carbon and nitrogen isotopic compositions ($\delta^{13}C$ and $\delta^{15}N$) and C/N of bulk leaves and purified Pheo *a* using the elemental analyzer coupled to isotope ratio mass spectrometry (Delta Plus XP) with a Conflo III interface (Thermo Finnigan, Bremen, Germany) for ultra-small-scale analysis (nano EA/IRMS) system (Isaji et al., 2020; Ogawa et al., 2010). In brief, a small piece of leaves (50–70 µg dry weight) was used for the bulk measurement. The purified Pheo *a* was dissolved in a 400 µL of trichloromethane (TCM). A portion of the TCM solution corresponding to about 3 µg of Pheo *a* (10–42 µL, depending on the Pheo *a* concentration) was transferred into a pre-cleaned tin capsule using a pre-cleaned glass syringe on a hot plate set at 80 ºC. The data were calibrated using three interlaboratory-consensus reference materials (standard name, $\delta^{13}C$, and $\delta^{15}N$: BG-A, –26.9‰, and –1.7‰; BG-P, –10.3‰, and +13.5‰; and BG-T, –20.8‰, and +8.7‰) (Tayasu et al., 2011) and three in-house reference materials (BG-LC-G, –13.4‰, and –5.4‰; BG-GC-G, –13.4‰, and –5.7‰; and SK-GC-V, +0.2‰, and +60.4‰). An in-house Chl *a* standard was also measured to assess reproducibility of the C/N ratios (n = 3, mean and standard deviation, 12.1 ± 0.6) prepared for ultra-small-scale measurements (Isaji et al., 2020). The analytical errors of the $\delta^{13}C$ and $\delta^{15}N$ measurements obtained by the repeated analyses were less than ±0.37‰ for $\delta^{13}C$ (n = 22, 1.1–6.9 µgC) and less than ±0.64‰ for $\delta^{15}N$ (n = 19, 0.14–0.9 µgN).

2.4 Purity assessment

Based on the observed C/N ratios of purified Chl *a* fractions by the nano EA/IRMS measurements, a mass-balance equation with respect to impurity being derived from sample matrix and/or procedural blank was written as follows.

$$C\ or\ N_{Observed} = C\ or\ N_{Expected} + C\ or\ N_{Impurity}. \quad (1)$$

Equation (1) was rewritten in terms of carbon (hereafter referred to as impurity carbon in percentage) as follows.

$$\frac{C_{Impurity}}{C_{Observed}} = \frac{C_{Observed} - C_{Expected}}{C_{Observed}} = 1 - \frac{C/N_{Expected} \times N_{Expected}}{C_{Observed}}, \quad (2)$$

Under the condition where all the nitrogen detected on EA/IRMS is derived from Chl *a* (i.e., $N_{Impurity} = 0$), Eq. (1) was rewritten in terms of nitrogen as follows.

$$N_{Observed} = N_{Expected}. \quad (3)$$

Substituting Eq. (3) for Eq. (2) yielded the following equation.

$$\frac{C_{Impurity}}{C_{Observed}} = 1 - \frac{C/N_{Expected} \times N_{Observed}}{C_{Observed}} = 1 - \frac{C/N_{Expected}}{C/N_{Observed}}. \quad (4)$$

Given that $C/N_{Expected}$ is 11.8 for Chl *a* (weight/weight, 55 carbon atoms and 4 nitrogen atoms) and the repeated nano EA/IRMS measurement of our in-house Chl *a* standard gives analytical error of C/N ± 1.2 (2σ), the analytically permissible range of the impurity carbon percentage was from –11% to 9%, corresponding to $C/N_{Observed}$ from 10.6 to 13.0, respectively. This was used as the criterion for sample Chl *a* purity in this study. It should be mentioned that the criterion is more relaxed compared to the stricter one when the EA/IRMS measurement was implemented at a larger scale (Isaji et al., 2020).

To identify and characterize impurity carbon in the purified Pheo *a* fractions, three additional assessments based on (i) diode array detector (DAD), (ii) Orbitrap MS, and (iii) GC/MS spectra were performed. Assessment (i) was subject to all eight samples, while assessment (ii) subject to 1952, 1968, 1973, 1982, and 1995 samples and assessment (iii) to 1952 and 1968 samples due to availability of leftover materials after CSRA. Experimental details and analytical settings of each assessment are found in Supplemental Information.

2.5 Radiocarbon measurements

The radiocarbon content is reported as $F^{14}C$ (Reimer et al., 2004). The present study derived $\Delta^{14}C$ (‰) from the reported $F^{14}C$ value as follows.

$$\Delta^{14}C = F^{14}C \times e^{\lambda(1950-x)} - 1, \quad (5)$$

where λ and *x* are the decay constant of ^{14}C ($1/8267 = 1.21 \times 10^{-4}$) and the year when ^{14}C was measured, respectively. $\Delta^{14}C$ is expressed in ‰, which is also formulated as follows (Stuiver and Polach, 1977).

$$\Delta^{14}C = \delta^{14}C - 2(\delta^{13}C + 0.025)(1 + \delta^{14}C). \quad (6)$$

where $\delta^{13}C$, $\delta^{14}C$, and $\Delta^{14}C$ are expressed in ‰ and carbon isotopic fractionations are internally corrected by $\delta^{13}C$ (Stuiver and Polach, 1977). The bulk leaf $\Delta^{14}C$ ($\Delta^{14}C_{Leaf}$) values of a small piece of leaves (3–4 mg dry weight) were determined using an accelerator mass spectrometer (AMS) at the Institute of Accelerator Analysis (Kanagawa, Japan; AMS lab code IAAA) in which analytical errors (1σ) were better than 4.0‰. The compound-specific radiocarbon analysis (CSRA) of Chl *a* ($\Delta^{14}C_{Chl}$) were conducted according to Haghipour et al., (2019). In brief, 16–40 μgC of purified Chl *a* fractions ($n = 8$) were submitted to CSRA. The dried Chl *a* samples were dissolved in 30 μL of dichloromethane. 15–30 μL of each sample was transferred into

Deleted: :

Deleted: ¶

Deleted: in the present study

Deleted: (

Deleted:)

Deleted: :

Deleted: δ14C1000

Deleted: →

Deleted: 5

Deleted: The amount of carbon in samples was >80 times larger than procedural blank (0.1–0.2 μgC) estimated in our previous studies (Ishikawa et al., 2015; Yamamoto et al., 2020).

a pre-cleaned (washed with DCM three times) tin capsule (3 mm diameter, 6 mm height, and 25 µL volume, P/N 84.9906.26, Lüdi Swiss, Switzerland) using a pre-cleaned glass syringe on a hot plate set at 80 ºC. The syringe transfer was repeated three times to increase recovery. The folded capsules were then placed on an autosampler, which is transferred into an elemental analyzer (Elementar, Handforth, UK) where they were combusted to gaseous CO_2 before being sent to a gas ion source/miniature carbon dating system (GIS/MICADAS) at Ion Beam Physics Laboratory, ETH Zürich (lab code ETH) in which analytical errors (1σ) were better than 8.1‰. Although the Chl *a* standards that have modern ^{14}C (i.e., $\Delta^{14}C$ >0‰) and dead ^{14}C (i.e., $\Delta^{14}C$ ~ –1,000‰) are commercially unavailable, we conducted a blank assessment for the entire procedure and found that the procedural blank has 0.32 ± 0.10 µgC (Fig. 2), which is smaller than that found in typical CSRA studies (e.g., Haghipour et al., 2019; Ishikawa et al., 2018). Even in the most extreme case where the wet chemistry blank $\Delta^{14}C$ was –1,000‰, the effect of the procedural blank on Chl *a* $\Delta^{14}C$ correction is smaller than the AMS analytical error (± 8‰, 1σ). The procedural blank assessment is detailed in Supplemental Information.

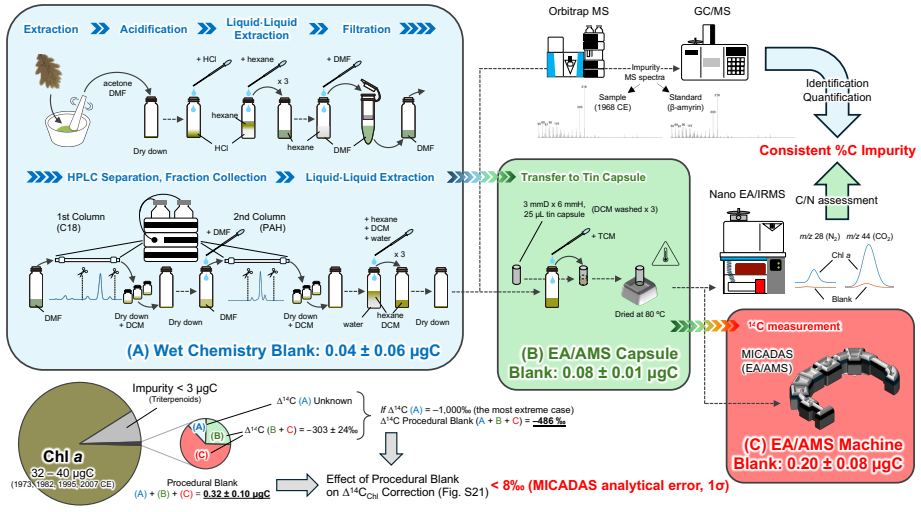

Figure 2: Workflow for Chl *a* sample preparation and its associated impurity and procedural blank assessments.

2.6 Model

We used $\Delta^{14}C$ data of atmospheric CO_2 and tree rings during 1950 and 2019 (monthly resolution, i.e., 12 data per year, n = 833) in the Northern Hemisphere Zone 1 (NH1), which covers aerial Switzerland, provided by Hua et al., (2022). The timeseries dataset (t = 1, 2, …, 833) consists of decimal-year time points and $\Delta^{14}C$ values (hereafter referred to as $\Delta^{14}C_{Atm\ (t)}$). The decimal years nearest to the times when *Quercus* samples were collected were identified (t = 32: 1952.625; t = 188:

1965.625; t = 197: 1966.375; t = 225: 1968.708; t = 283: 1973.542; t = 391: 1982.542; t = 545: 1995.375; and t = 691: 2007.542). The difference in decimal years between the *Quercus* sample collection time and their nearest time t was 0.008 ± 0.03 (n = 8, equivalent to 2.9 ± 9.9 days).

To interpret observed $\Delta^{14}C$ values of Chl *a*, a two-pool model developed for the soil carbon pool (Koarashi et al., 2012) was applied to our dataset with a modification. We considered two different carbon pools as follows:

$$F_{Q(t+1)} = F_{Q(t)}\left(1 - 1/T_Q - \lambda\right) + 1/T_Q\, F_{Atm(t)}, \quad (7)$$

$$F_{S(t+1)} = F_{S(t)}\left(1 - 1/T_S - \lambda\right) + 1/T_S\, F_{Atm(t)}, \quad (8)$$

where F is the $F^{14}C$ value, and $F_{Q(t)}$, T_Q, $F_{S(t)}$, and T_S are the $F^{14}C$ at time t and turnover time of *Quercus* leaf and soil carbon pools, respectively. We assumed that the Chl *a* compound is a mixture of these two carbon pools, and its F value is formulated as follows:

$$F_{Chl(t)} = P_Q F_{Q(t)} + P_S F_{S(t)}, \quad (9)$$

where $F_{Chl\,(t)}$ is $F^{14}C$ of Chl *a* at time t and P_Q and P_S are proportional size of *Quercus* leaf and soil organic matter, respectively ($P_Q + P_S = 1$). *Quercus* is a deciduous tree with faster and less variable carbon turnover (i.e., 1–2 years, Ichie et al., 2013) than the soil (van der Voort et al., 2019). Therefore, in the model, T_Q was set at constant 1.5 years and T_S was allowed to vary between 0 and 3,000 years. P_S was allowed to vary between 0% and 30%. The stepwise model was run with intervals of 100 years and 0.1% for T_S (31 models) and P_S (301 models), respectively (31 × 301 = 9,331 models in total) to reconstruct radiocarbon trajectories for each model from 1950 to 2019.

To constrain T_S (i.e., turnover time of the soil pool contributing to Chl *a*) and P_S (percentage of the soil pool contributing to Chl *a*) at time t using the observed and modelled $\Delta^{14}C_{Chl\,(t)}$ ($\Delta^{14}C_{Chl,\,observed\,(t)}$ and $\Delta^{14}C_{Chl,\,modelled\,(t)}$, respectively) values, we computed their absolute difference at each of the eight years (i.e., 1952, 1965, 1966, 1968, 1973, 1982, 1995, and 2007) for mutually independent models as follows:

$$\Delta\Delta^{14}C = \left|\Delta^{14}C_{Chl,\ observed\,(t)} - \Delta^{14}C_{Chl,\ modelled\,(t)}\right|. \quad (10)$$

The closer to $\Delta\Delta^{14}C$ = 0, the more plausible the T_S and P_S expected. Therefore, the T_S and P_S values that gave the smallest $\Delta\Delta^{14}C$ values were explored for each of the eight years among the 9,331 models (van der Voort et al., 2019).

All the statistical analyses and graphing were performed using MATLAB 2025b (MathWorks, USA).

3 Results

The $\delta^{13}C$ and $\delta^{15}N$ values of bulk leaves ($\delta^{13}C_{Leaf}$ and $\delta^{15}N_{Leaf}$) ranged from –28.2‰ to –24.1‰ and from –5.7‰ to +1.4‰, respectively (Table 1). The C/N weight ratios of bulk leaves ranged from 17.2 to 23.0 and were not significantly different between *Q. pubescens* and *Q. petraea* (Wilcoxon rank sum test, $p > 0.99$). The $\delta^{13}C$ and $\delta^{15}N$ values of Chl *a* ($\delta^{13}C_{Chl}$ and

Deleted: :
Deleted: 6
Deleted: 7
Deleted: fraction ($\Delta^{14}C/1000 + 1$)
Deleted: λ is the decay constant of ^{14}C (1.21×10^{-4}),
Deleted: ^{14}C fraction
Deleted: :
Deleted: 8
Deleted: the ^{14}C fraction
Deleted: 0
Deleted: 0
Deleted: :
Deleted: 9
Deleted: a

$\delta^{15}N_{Chl}$) ranged from –30.1‰ to –25.4‰ and from –3.0‰ to +2.7‰, respectively (Table 1). There were significantly positive correlations between $\delta^{13}C_{Leaf}$ and $\delta^{13}C_{Chl}$ values (n = 8, $\delta^{13}C_{Leaf}$ = +0.71 $\delta^{13}C_{Chl}$ – 6.73, r^2 = 0.70, p = 0.006) (Fig. 3a) and between $\delta^{15}N_{Leaf}$ and $\delta^{15}N_{Chl}$ values (n = 8, $\delta^{15}N_{Leaf}$ = +0.63 $\delta^{15}N_{Chl}$ – 1.57, r^2 = 0.72, p = 0.005) (Fig. 3b).

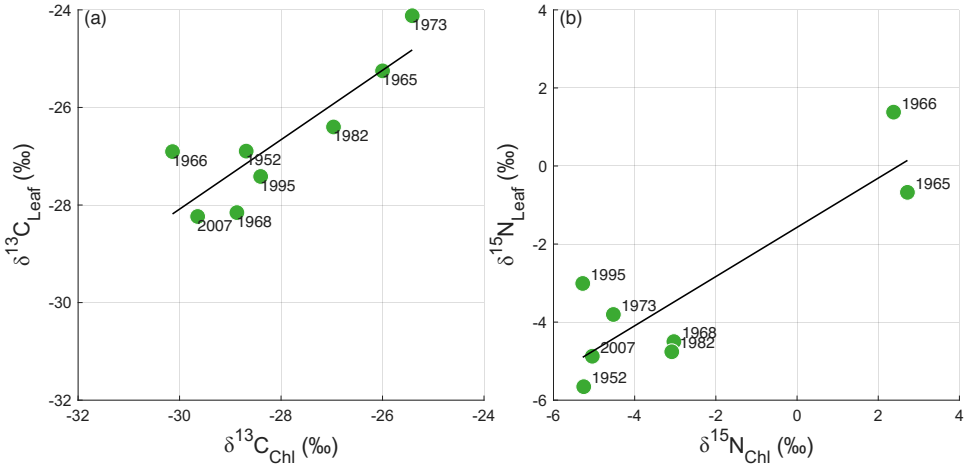

Figure 3: Plots for (a) $\delta^{13}C_{Leaf}$ and $\delta^{13}C_{Chl}$ and (b) $\delta^{15}N_{Leaf}$ and $\delta^{15}N_{Chl}$ (n = 8). Numbers beside circles indicate collection years (CE). Regression lines ($\delta^{13}C_{Leaf}$ = +0.71 $\delta^{13}C_{Chl}$ – 6.73, r^2 = 0.70, p = 0.006; $\delta^{15}N_{Leaf}$ = +0.63 $\delta^{15}N_{Chl}$ – 1.57, r^2 = 0.72, p = 0.005) are shown.

The C/N weight ratios of Chl *a* and impurity carbon % in 1973, 1982, 1995, and 2007 were from 10.7 to 12.7 and from –10 to 7% (n = 4), respectively, which were within the criterion (i.e., 10.6–13.0 and –11 to 9%). On the other hand, C/N and impurity carbon % of Chl *a* in 1952, 1963, 1966, and 1968 (13.6–16.3 and 13–27%, respectively) (n = 4) were out of the permissible range (Table 1). GC/MS analysis of selected samples (1952 and 1968 CE) identified that a minor amount of pentacyclic triterpenoids (30 carbon atoms and no nitrogen) remained with Chl *a* even after two-step HPLC separation followed by liquid-liquid extraction until CSRA measurements, which likely increased the resultant C/N ratios (Figs. S8–17). The carbon contents derived from the hydrophobic triterpenoids (simiarenol, β-amyrin, and their derivatives; 13% in 1952 and 11% in 1968) showed good agreement with the impurity carbon percentage estimated by Eq. (4) (13% in 1952 and 16% in 1968). The differences between the two estimates (0.2% and 4.4% for the 1952 and 1968 Pheo *a* samples, respectively) were smaller than our purity criterion (< 4.5%, 1σ) based on the C/N analytical error. Therefore, there is no evidence that the impurity in the purified Pheo *a* samples has carbon other than simiarenol and β-amyrin, which were not derived from column bleed nor organic solvents that had been potentially made from fossil-fuel products being depleted in ^{14}C. The native triterpenoids are produced by plants such as a leaf wax and are expected to have $\Delta^{14}C$ values close to those of either atmospheric CO_2 at the time of leaf collection, bulk leaf, or Chl *a*, which does not make our conclusions unrealistic.

Deleted: 2
Deleted: 2
Deleted: 2
Deleted: .
Deleted: 6
Deleted: 3
Deleted: 2
Deleted: ,
Deleted: 3

The $\Delta^{14}C$ values of the bulk archival leaves (i.e., $\Delta^{14}C_{Leaf}$) followed trajectory of the bomb carbon signal of atmospheric CO_2 (Fig. 4). The $\Delta^{14}C_{Leaf}$ values were lower by 4.4 to 44.6‰ than the atmospheric $\Delta^{14}C$ at time t ($\Delta^{14}C_{Atm\,(t)}$) when the leaf samples were collected. The $\Delta^{14}C_{Leaf}$ value in 1952, which was sampled before the first hydrogen-bomb testing Operation Ivy was conducted in November 1952, was below 0‰ (–46.8‰, $\Delta^{14}C_{Atm\,(t)}$ = –25.3‰). Soon after the Partial Test Ban Treaty (PTBT) took effect in 1963, the $\Delta^{14}C_{Leaf}$ value in 1965 (+746.8‰, $\Delta^{14}C_{Atm\,(t)}$ = +791.4‰) was highest in our dataset, followed by +689.0‰ ($\Delta^{14}C_{Atm\,(t)}$ = +701.6‰) in 1966, +560.2‰ ($\Delta^{14}C_{Atm\,(t)}$ = +578.1‰) in 1968, and have continuously decreased onward (Table 1). The $\Delta^{14}C$ values of Chl *a* ($\Delta^{14}C_{Chl}$) were all lower than their corresponding $\Delta^{14}C_{Leaf}$ values (Fig. 4). The highest $\Delta^{14}C_{Chl}$ value was found in 1966 (+624.1‰) rather than 1965 (+599.7‰) when the $\Delta^{14}C_{Leaf}$ value was highest. There was a significantly positive correlation between $\Delta^{14}C_{Leaf}$ and $\Delta^{14}C_{Chl}$ values (n = 8, $\Delta^{14}C_{Leaf}$ = +1.10 $\Delta^{14}C_{Chl}$ + 34.8, r^2 = 0.99, p < 0.001). The difference between $\Delta^{14}C_{Chl}$ and $\Delta^{14}C_{Leaf}$ was greatest in 1965 (–147‰), followed by 1963, 1966, and 1973 (–65‰) when $\Delta^{14}C$ of atmospheric CO_2 was >+400‰ (Fig. 4). In contrast, this difference compressed through time, 1982 (–46‰), 1995 (–40‰), and 2007 (–38‰) when $\Delta^{14}C$ of atmospheric CO_2 continuously decreased due to oceanic and biospheric $^{14}CO_2$ exchange as well as ^{14}C-free CO_2 dilution via fossil fuel combustion (Fig. 4). The difference was smallest in 1952 (–33‰) which is before the first hydrogen-bomb testing (November 1952). These differences were all greater than the CSRA analytical error (2σ = 16‰) and were not significantly different between *Q. pubescens* and *Q. petraea* (Wilcoxon rank sum test, p = 0.39).

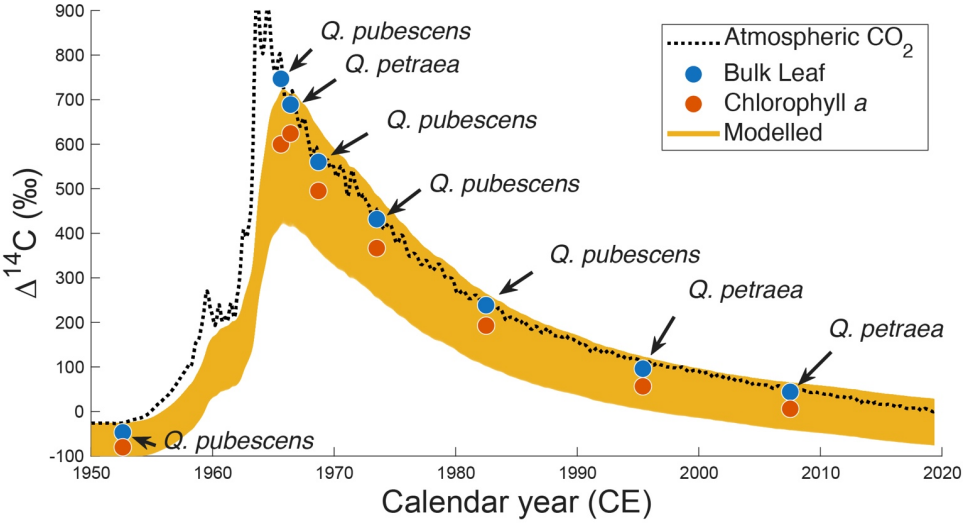

Figure 4: Change in $\Delta^{14}C$ values of atmospheric CO_2 (black line, data from Northern Hemisphere (NH) zone 1, Hua et al., 2022), those of bulk leaves (blue circle) and their corresponding Chl *a* (red circle), and modelled trajectories with different conditions of soil proportion (T_S, boundaries: 0–30%) and turnover time (T_S, boundaries: 0–3,000 years) (total 9,331 orange lines).

To minimize the effect of impurity on the estimation of soil carbon contribution to Chl *a*, the model results after 1972 CE (n = 4) were only shown in Figs. 4 and 5. The difference between observed and modelled $\Delta^{14}C_{Chl}$ values ($\Delta\Delta^{14}C$) on the biplot space of soil turnover time (T_S, years) versus soil proportion (P_S, %) varied depending on years when the samples were collected (Fig. 5). The most plausible models for the four years that gave the smallest $\Delta\Delta^{14}C$ (< 0.01‰) constrained P_S range as 15–19% (17 ± 2%) (n = 4), while T_S range longer than 1,000 years (Table 1). The integrated heatmap that shows the arithmetic mean of the $\Delta\Delta^{14}C$ values from the four years gave the most plausible P_S as 15.4% while T_S unconstrained (Fig. 6). It should be mentioned that the model results using all Chl *a* data including those before 1972 CE (n = 4) indicated similar estimates ($\Delta\Delta^{14}C$ < 0.03‰, P_S range 11–29%, and P_S mean and standard deviation 17 ± 6%) (Figs. S19 and S20). We also carried out a sensitivity analysis by tweaking the T_Q values from 0.5 to 5.0 years, and no substantial change was observed (Fig. S21), suggesting that the model estimates are insensitive to the T_Q values in this range. It should be noted that the leaf turnover time ≥ 5.0 years is unlikely because such an endmember cannot explain the 1965 and 1966 $\Delta^{14}C_{Chl}$ data (Fig. S25), which should be lower than the endmember $\Delta^{14}C$ to satisfy the mass balance.

Deleted: 3
Deleted: 4
Deleted: 2
Deleted: 3
Deleted: 26
Deleted: 9
Deleted: 5
Deleted: 3
Deleted: 5
Deleted: 0
Deleted: 8
Deleted: 8
Deleted: 5
Deleted: 16

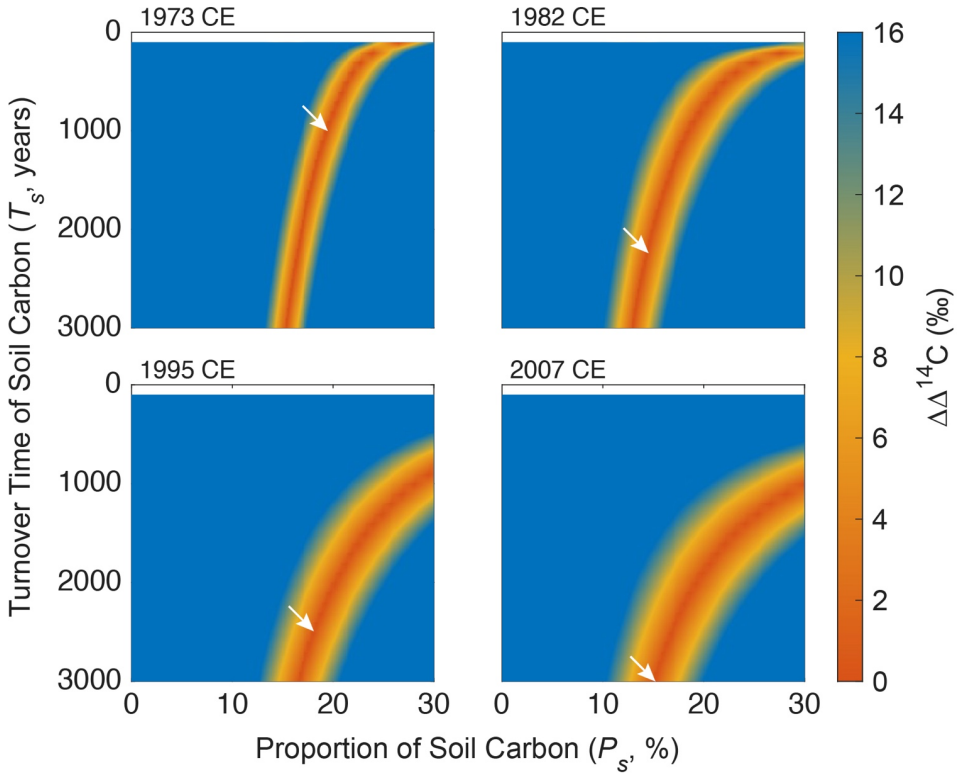

405

Figure 5: Heatmaps of the difference ($\Delta\Delta^{14}C$) between observed and modelled $\Delta^{14}C_{Chl}$ values on a biplot for soil turnover time (T_s, years) versus soil proportion (P_s, %) for each of the four samples collected in different years. The $\Delta\Delta^{14}C$ value larger than the 2σ analytical error of CSRA (>16‰) was not considered in this plot. The white arrows denote the smallest $\Delta\Delta^{14}C$ values (i.e., the most plausible models).

Deleted: 4

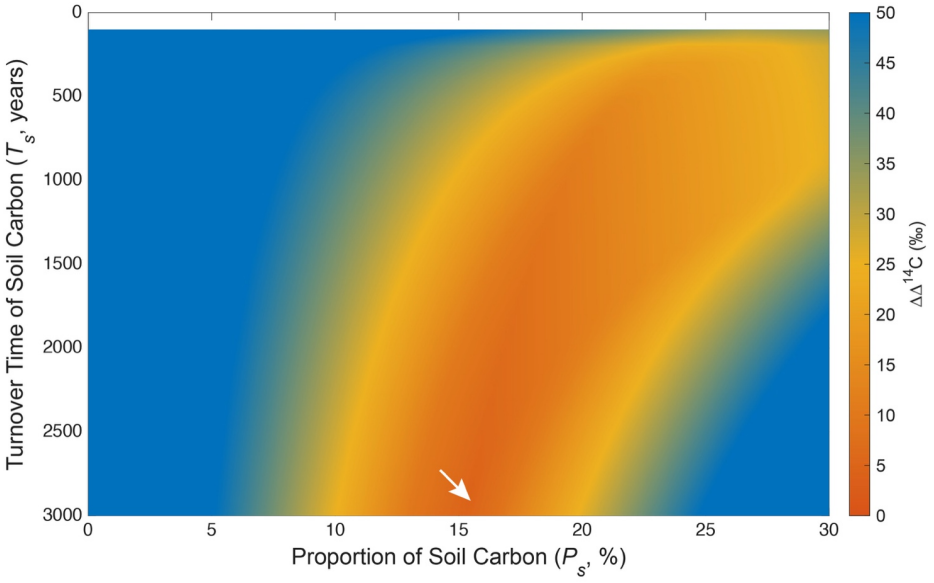

Figure 6: The $\Delta\Delta^{14}C$ heatmap that overlayed all the four heatmaps in Figure 4. The arithmetic mean of the $\Delta\Delta^{14}C$ values from the four years are shown. The white arrow denotes the smallest $\Delta\Delta^{14}C$ value (i.e., the most plausible model).

Deleted: 5

Deleted: eight

4 Discussion

4.1 Retrospective analysis using bomb-radiocarbon signals

The present study indicates that Chl *a*, which is an essential compound for photosynthesis in a variety of autotrophs, involves carbon atoms that are not directly routed from atmospheric CO_2 (Fig. 7). Atmospheric $^{14}CO_2$ concentrations in Northern Hemisphere tend to be higher in winter and spring when the troposphere is well-mixed with the stratosphere to which a significant amount of bomb-derived ^{14}C was injected during the 1950s and 1960s (Randerson et al., 2002). Among the eight years when our leaf samples were collected, intra-year variations in $\Delta^{14}CO_2$ values reached up to 100‰ in 1965, followed by 60‰ in 1966, and <30‰ in 1968 (Hua et al., 2022), all of which were excluded from our model in the interest of the Chl *a* purity. The bomb ^{14}C seasonality is overlapped but not perfectly concurrent with *Quercus* oak phenology where the leaf growth and Chl *a* production are maximal in spring and summer (Mészáros et al., 2007). If our *Quercus* leaf samples, which had been collected from late spring (May) to late summer (September), were predominantly made from ^{14}C-enriched carbon available in the springtime, their $\Delta^{14}C_{Leaf}$ values should be higher than atmospheric $\Delta^{14}C$ values at time *t* ($\Delta^{14}C_{Atm\ (t)}$) of the respective

Deleted: 6

year. Nevertheless, the $\Delta^{14}C_{Leaf}$ was rather always lower than $\Delta^{14}C_{Atm\,(t)}$, which is not explainable with the single carbon source. The Chl *a* compound brings carbon being depleted in ^{14}C by 33.4 to 147.1‰ relative to the bulk leaf. Since the Chl *a* concentration in the *Quercus* oak is at most 1–2% of the total weight in their leaves (Rodríguez-Calcerrada et al., 2008), its contribution to the difference between $\Delta^{14}C_{Leaf}$ and $\Delta^{14}C_{Atm\,(t)}$ is approximately <30%. Therefore, it is demonstrated that Chl *a* is not the only compound that lowers $\Delta^{14}C_{Leaf}$ values. By employing the high-resolution CSRA methodology, we found that there exists other ^{14}C-depeleted compound(s) that cannot be unveiled by conventional bulk radiocarbon measurements.

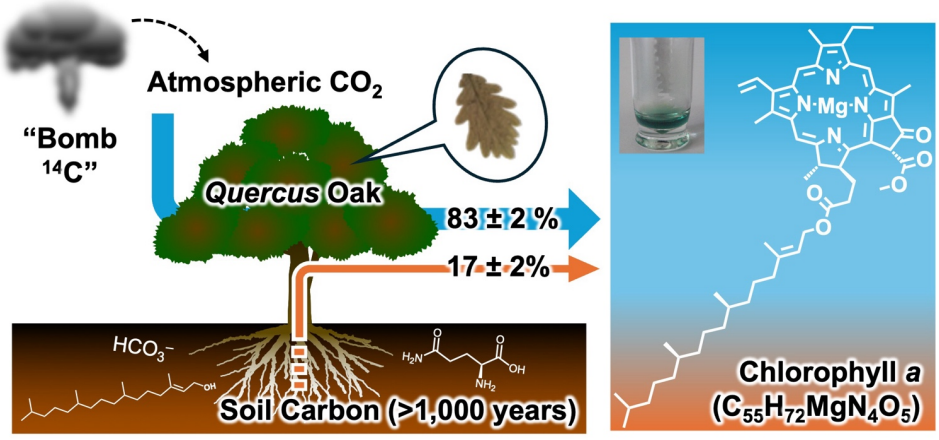

Figure 7: Schematic representation of this study.

Deleted: 6

The $\Delta^{14}C_{Chl}$ value consistently lower than the $\Delta^{14}C_{Leaf}$ value throughout the 50-year-long chronology suggests that very old carbon is derived from elsewhere. Indeed, the difference between $\Delta^{14}C_{Chl}$ and $\Delta^{14}C_{Leaf}$ values is greater in the 1960s and 1970s (when the bomb-derived radiocarbon remained in the atmosphere at high concentrations) than in the others. The results cannot be explained without considering another source of carbon that has turnover time longer than the atmosphere. The $\Delta^{14}C_{Chl}$ values after the 1970s suggest the scale of the turnover time of this additional carbon source. If the source's turnover time was decadal to centennial scales, its $\Delta^{14}C$ value should have become higher than atmospheric $\Delta^{14}C$ values at some point onward. For example, the source's turnover time 10, 50, and 100 years makes its $\Delta^{14}C$ endmember higher than atmospheric $\Delta^{14}C$ after 1973, 1989, and 1999 CE, respectively (Gaudinski et al., 2000). Under the condition where this additional carbon source contributes to the Chl *a*, the $\Delta^{14}C_{Chl}$ values should be always higher than atmospheric $\Delta^{14}C$. Obviously, this was not the case in the present study, nor consistent with our previous study where Japanese blue oak *Quercus glauca* collected in 2013 showed a $\Delta^{14}C_{Chl}$ value 37‰ lower than its $\Delta^{14}C_{Leaf}$ (Ishikawa et al., 2015). Our data collectively suggest that the additional carbon source has turnover time longer than 100 years. Although *Quercus* oak trees can live >100 years, forests accommodating such

a long-living tree are rare in Europe due to frequent human disturbances (Martin-Benito et al., 2021). Therefore, such a carbon source with >100-year turnover time is, most likely, in rhizosphere.

4.2 Soil carbon contribution to Chl *a*

The most plausible (i.e., smallest $\Delta\Delta^{14}C$) two-pool models estimated contributions of soil carbon to Chl *a* in the *Quercus* leaf (i.e., P_S) significantly greater than 0% (mean and standard deviation, 17 ± 2%). We designed our indeterministic model not to deduce a unique algebraic solution from the differential equations, but to induce the most parsimonious and the least unlikely constraint from available data. Although the four years (1973, 1982, 1995, and 2007 CE) that met our purity criterion did not hold as large a $\Delta^{14}C$ offset as the other four years (1952, 1965, 1966, and 1968 CE), all of them showed consistent P_S values. Even if our estimates were affected by currently unconsidered factors, the most plausible P_S values would not be <10% in all the four years (Fig. 6) unless the soil turnover time T_S was extended to longer than 3,000 years, which is biogeochemically improbable. We acknowledge that the T_S values (1,000–3,000 years) were less constrained than P_S in our model, leaving a key question "how deep and old carbon in soils is incorporated into plants" open to debate.

van der Voort et al., (2019) showed that the typical turnover time of surface soil (0-5 cm) in Switzerland is 14–410 years. Considering the *Quercus* trees grow their root down to 700 cm below ground level (David et al., 2013), it is most likely that they acquire carbon below the soil organic layer via root uptake for synthesizing the Chl *a*. The turnover time of such soil carbon (i.e., T_S) was no shorter than 1,000 years in our most plausible model, which roughly corresponds to the soil deeper than 20 cm (van der Voort et al., 2019). It might be somewhat surprising that carbon in Chl *a* is partly originated from such a deep soil layer, as organic carbon content generally decreases with soil depth (van der Voort et al., 2019). The carbon pool with turnover times on the order of millennium is believed to be tightly stabilized by minerals and hardly accessed by plants or microbes. Therefore, such carbon is apparently the last candidate of a building block for the Chl *a* compound in *Quercus* oak among all other carbon available in the rhizosphere. The present study shows the very first but preliminary evidence of the millennial-aged carbon contributing to Chl *a*, which contrasts sharply with the current pedological paradigm. However, our observation is associated with analytical (lack of working standards) and methodological (unconstrained T_S values) limitations as mentioned earlier. Furthermore, it is challenging to estimate the exact soil depth where the old carbon is sourced because it would depend on temperature, precipitation, soil type, and aboveground vegetation, all of which are highly uncertain and beyond the scope of this study. In fact, $\delta^{13}C$ and $\delta^{15}N$ values varied greatly among the eight *Quercus* leaf samples, suggesting that their growing condition was quite different from each other. This would also be one of the reasons the estimated P_S and T_S varied. Further investigations are needed to demonstrate the validity of our results, the potential significance of this process, and the broader relevance with respect to carbon cycling.

Direct uptake of Chl *a* from soil through root would be unlikely due to its hydrophobicity, phototoxicity, and instability outside the cell (Matile et al., 1999). *Quercus* is one of the oak trees that develops a symbiosis with ectomycorrhizal fungi (Smith and Read, 2008). It is possible that the ectomycorrhizal symbiosis plays a critical role in breaking down organo-mineral complex in soils (Landeweert et al., 2001) and mobilizing carbon as inorganic forms such as HCO_3^- or as hydrophilic compounds such

Deleted: 9
Deleted: 5
Deleted: 3

as phytol or amino acids that can permeate fine roots of their host plants (Jones et al., 2005, 2009). Although these organic compounds are mainly derived from photosynthetic products, their $\Delta^{14}C$ values near the interface between fine roots and ectomycorrhizal fungi might be extremely low (Trumbore, 2000). It is reported that amino acids and monoterpenes are translocated via xylem with water to synthesize a variety of organic compounds including storage proteins or secondary metabolites (Martin et al., 2002; Nabais et al., 2005). Therefore, there is no reason to conclude that Chl *a* is the only organic compound to which soil-derived carbon is incorporated, as discussed earlier with respect to $\Delta^{14}C_{Atm\ (t)}$, $\Delta^{14}C_{Leaf}$, and $\Delta^{14}C_{Chl}$ values. If this was the case, radiocarbon age and provenance within and among compounds in a single tree would be more diverse than previously thought.

Despite no direct evidence on what kind of soil carbon, either organic or inorganic, contributes to the Chl *a* biosynthesis in chloroplast, previous isotope-labeling studies using ^{13}C, ^{14}C, and ^{15}N showed that plants do take up organic carbon and nitrogen from the soil (Moran-Zuloaga et al., 2015; Rasmussen et al., 2010). Given that some organic nitrogen in plants is derived from soil (Näsholm et al., 1998), so is carbon would be unsurprising. However, microbial remineralization of the labile and labeled organic matter such as amino acids before root uptake particularly evident in agricultural soils is controversial (Farzadfar et al., 2021). Furthermore, it is highly uncertain about the fate of such soil-derived organic matter in the plant metabolism in which Chl *a* plays a significant role (Masuda and Fujita, 2008). As reported in Cress *Arabidopsis thaliana* (Ischebeck et al., 2006) and cyanobacteria *Synechocystis* sp. (Vavilin and Vermaas, 2007), the side chain (phytol, 20 carbon compound) of the Chl *a* (55 carbon compound) could be salvaged from its catabolic pathway. It is believed that the remaining chlorophyllide *a* (35 carbon compound) is not recycled because the compound is photo-toxic for plant cells (Matile et al., 1999). This leads us to a hypothesis that plants uptake nitrogen-rich amino acids such as glutamine from rhizosphere, use its amide as a nitrogen source, and transfer the resulting glutamic acid or carbon skeleton to the Chl *a* biosynthesis. Although speculative, it is possible that approximately 30% of chlorophyllide *a* or half of phytol derived from the rhizosphere explain the P_S value (17 ± 2%) constrained in our two-pool model.

Moved (insertion) [1]

Moved up [1]: Given that some organic nitrogen in plants is derived from soil (Näsholm et al., 1998), so is carbon would be unsurprising.

Deleted: 9

Deleted: 5

5 Conclusions and implications

Our current understanding about global carbon cycle does not take account of a feedback pathway from rhizosphere to biosphere. The findings of this study may not be limited to *Quercus* but applicable to other vascular plants. Given that 10–20% of previously overlooked carbon is recovered from the sequestered soil pool, the current picture of carbon cycling between biosphere and rhizosphere would be considerably revised. Furthermore, if other compounds constituting the leaves are also old in age, the carbon supplied from the rhizosphere to the biosphere deserves to be considered qualitatively. The two major carbon sources for terrestrial plants, atmosphere and rhizosphere, offer us a unique opportunity to analytically solve the two-pool model using $\Delta^{14}C$ values. Our finding may also be relevant to aquatic photoautotrophs where the $\Delta^{14}C$ values of Chl *a* and its derivatives have been used as tools to determine the age of sediment formation and their depositional processes (Kusch

Deleted: budget

Deleted: via terrestrial primary production

Deleted: found in

et al., 2010; Yamamoto et al., 2020). The results raise an intriguing question of whether these aquatic photoautotrophs partially recycle carbon from sources other than ambient CO_2 (i.e., dissolved inorganic carbon) to synthesize Chl *a*.

The retrospective analysis in this study was made possible by hydrogen-bomb tests in the atmosphere during the Cold War period that unintentionally created a natural laboratory on the surface Earth for tracing centennial-scale carbon cycle (Oeschger et al., 1975). Instead of adding ^{14}C-labeled carbon to rhizosphere, we demonstrated the naturally labeled ^{14}C signal in atmosphere as a promising tracer for carbon trade between biosphere and rhizosphere. The bomb radiocarbon dating has been widely applied for annually growing biological samples, such as tree rings (Hua et al., 2022), wines (Burchuladze et al., 1989), bivalve shells (Kubota et al., 2018), and shark vertebrae (Hamady et al., 2014), to reconstruct their recent past chronology. On the other hand, since Eglinton et al., (1996) first proposed the CSRA methodology, its application to a variety of organic compounds has significantly contributed to advancing biogeochemical research (e.g., Eglinton et al., 1997; Ingalls and Pearson, 2005; Kruger et al., 2023; Mollenhauer et al., 2007; Ohkouchi et al., 2002). This advance has been established upon the experimental and instrumental developments that enabled to downsize carbon amounts as well as procedural blank and to diversify targeted organic compounds for CSRA (e.g., Haghipour et al., 2019; Ishikawa et al., 2018). In line with this context, the present study sheds light on botanical and other biological collections in herbariums or museums as a chronological recorder promising for CSRA. In addition to already existing applications mentioned above, the present study will be able to open a new research frontier of the CSRA biogeochemistry.

Appendices

Not applicable.

Code, data, or code and data availability

Should the manuscript be accepted, the data supporting the results will be archived in Figshare.

Supplement link

The link to the supplement will be included by Copernicus, if applicable.

Team list

Not applicable.

Author contributions

NFI, TSvdV, and TIE designed the study. NFI and RN collected leaves from archive specimens. NFI and HS prepared chlorophyll *a*. NFI, NOO, and NO conducted C/N and stable isotope measurements. NFI, NH, and LW conducted radiocarbon measurements. NFI analyzed data and wrote the first draft of the manuscript with input from HS, NOO, and NO. All the authors participated in discussion and approved the final manuscript.

Competing interests

The authors declare that they have no conflicts of interest.

Disclaimer

Not applicable.

Acknowledgements

We thank Kentaro Shimizu for technical advice, Franziska Schmid for laboratory assistance, Atsushi Urai, Thomas Blattmann, Yuta Isaji, Kohei Sakamoto, Yusuke Tsukatani, Kenji Suetsugu, and Yoshinori Takano for insightful discussion, Toshiki Koga for helping with the Orbitrap MS analysis, and two anonymous referees for valuable comments and constructive suggestions on an early version of the manuscript.

Deleted: Richard Baxter and Melissa Schwab for helping field work, Nadine Keller and

Deleted: and

Financial support

This study was supported by the JSPS Overseas Research Fellowship (2016-214) and Grants-in-Aid for Scientific Research (19K22463).

Review statement

The review statement will be added by Copernicus Publications listing the handling editor as well as all contributing referees according to their status anonymous or identified.

References

Burchuladze, A. A., Chudý, M., Eristavi, I. V, Pagava, S. V, Povinec, P., Šivo, A., and Togonidze, G. I.: Anthropogenic ^{14}C variations in atmospheric CO_2 and wines, Radiocarbon, 31, 771–776, https://doi.org/10.1017/S0033822200012388, 1989.

Cahanovitc, R., Livne-Luzon, S., Angel, R., and Klein, T.: Ectomycorrhizal fungi mediate belowground carbon transfer between pines and oaks, ISME J., 16, 1420–1429, https://doi.org/10.1038/s41396-022-01193-z, 2022.

Carbone, M. S., Czimczik, C. I., Keenan, T. F., Murakami, P. F., Pederson, N., Schaberg, P. G., Xu, X., and Richardson, A. D.: Age, allocation and availability of nonstructural carbon in mature red maple trees, New Phytol., 200, 1145–1155, https://doi.org/10.1111/nph.12448, 2013.

Clemmensen, K. E., Bahr, A., Ovaskainen, O., Dahlberg, A., Ekblad, A., Wallander, H., Stenlid, J., Finlay, R. D., Wardle, D. A., and Lindahl, B. D.: Roots and associated fungi drive long-term carbon sequestration in boreal forest, Science, 340, 1615–1618, https://doi.org/10.1126/science.1231923, 2013.

David, T. S., Pinto, C. A., Nadezhdina, N., Kurz-Besson, C., Henriques, M. O., Quilhó, T., Cermak, J., Chaves, M. M., Pereira, J. S., and David, J. S.: Root functioning, tree water use and hydraulic redistribution in *Quercus suber* trees: A modeling approach based on root sap flow, Forest Ecol. Manag., 307, 136–146, https://doi.org/10.1016/j.foreco.2013.07.012, 2013.

Eglinton, T. I., Aluwihare, L. I., Bauer, J. E., Druffel, E. R. M., and McNichol, A. P.: Gas chromatographic isolation of individual compounds from complex matrices for radiocarbon dating, Anal. Chem., 68, 904–912, https://doi.org/10.1021/ac9508513, 1996.

Eglinton, T. I., Benitez-Nelson, B. C., Pearson, A., McNichol, A. P., Bauer, J. E., and Druffel, E. R. M.: Variability in radiocarbon ages of individual organic compounds from marine sediments, Science, 277, 796–799, https://doi.org/10.1126/science.277.5327.796, 1997.

Farzadfar, S., Knight, J. D., and Congreves, K. A: Soil organic nitrogen: an overlooked but potentially significant contribution to crop nutrition, Plant and Soil, 462, 7–23, https://doi.org/10.1007/s11104-021-04860-w, 2021.

Gaudinski, J. B., Trumbore, S. E., Davidson, E. A., and Zheng, S.: Soil carbon cycling in a temperate forest: Radiocarbon-based estimates of residence times, sequestration rates and partitioning of fluxes, Biogeochemistry, 51, 33–69, https://doi.org/10.1023/A:1006301010014, 2000.

Goodwin, P. B.: Molecular size limit for movement in the symplast of the Elodea leaf, Planta, 157, 124–130, https://doi.org/10.1007/BF00393645, 1983.

Haghipour, N., Ausin, B., Usman, M. O., Ishikawa, N., Wacker, L., Welte, C., Ueda, K., and Eglinton, T. I.: Compound-specific radiocarbon analysis by Elemental Analyzer–Accelerator Mass Spectrometry: precision and limitations, Anal. Chem., 91, 2042–2049, https://doi.org/10.1021/acs.analchem.8b04491, 2019.

Hamady, L. L., Natanson, L. J., Skomal, G. B., and Thorrold, S. R.: Vertebral bomb radiocarbon suggests extreme longevity in white sharks, PLoS ONE, 9, 1–8, https://doi.org/10.1371/journal.pone.0084006, 2014.

Hua, Q., Barbetti, M., Zoppi, U., Fink, D., Watanasak, M., and Jacobsen, G. E.: Radiocarbon in tropical tree rings during the Little Ice Age, Nucl. Instrum. Methods Phys. Res. B., 223–224, 489–494, https://doi.org/10.1016/j.nimb.2004.04.092, 2014.

Hua, Q., Turnbull, J. C., Santos, G. M., Rakowski, A. Z., Ancapichún, S., De Pol-Holz, R., Hammer, S., Lehman, S. J., Levin, I., Miller, J. B., Palmer, J. G., and Turney, C. S. M.: Atmospheric radiocarbon for the period 1950-2019, Radiocarbon, 64, 723–745, https://doi.org/10.1017/RDC.2021.95, 2022.

Ichie, T., Igarashi, S., Yoshida, S., Kenzo, T., Masaki, T., and Tayasu, I.: Are stored carbohydrates necessary for seed production in temperate deciduous trees?, J. Ecol., 101, 525–531, https://doi.org/10.1111/1365-2745.12038, 2013.

Ingalls, A. and Pearson, A.: Ten years of compound-specific radiocarbon analysis, Oceanography, 18, 18–31, https://doi.org/10.5670/oceanog.2005.22, 2005.

Isaji, Y., Ogawa, N. O., Boreham, C. J., Kashiyama, Y., and Ohkouchi, N.: Evaluation of $\delta^{13}C$ and $\delta^{15}N$ uncertainties associated with the compound-specific isotope analysis of geoporphyrins, Anal. Chem., 92, 3152–3160, https://doi.org/10.1021/acs.analchem.9b04843, 2020.

Ischebeck, T., Zbierzak, A. M., Kanwischer, M., and Dörmann, P.: A salvage pathway for phytol metabolism in *Arabidopsis*. J. Biol. Chem., 281, 2470–2477, https://doi.org/10.1074/jbc.M509222200, 2006.

Ishikawa, N. F., Itahashi, Y., Blattmann, T. M., Takano, Y., Ogawa, N. O., Yamane, M., Yokoyama, Y., Nagata, T., Yoneda, M., Haghipour, N., Eglinton, T. I., and Ohkouchi, N.: Improved method for isolation and purification of underivatized amino acids for radiocarbon analysis. Anal. Chem., 90, 12035–12041, https://doi.org/10.1021/acs.analchem.8b02693, 2018.

Ishikawa, N. F., Yamane, M., Suga, H., Ogawa, N. O., Yokoyama, Y., and Ohkouchi, N.: Chlorophyll *a*-specific $\Delta^{14}C$, $\delta^{13}C$ and $\delta^{15}N$ values in stream periphyton: Implications for aquatic food web studies, Biogeosciences, 12, 6781–6789, https://doi.org/10.5194/bg-12-6781-2015, 2015.

Jones, D. L., Healey, J. R., Willett, V. B., Farrar, J. F., and Hodge, A.: Dissolved organic nitrogen uptake by plants - An important N uptake pathway? Soil Biol. Biochem., 37, 413–423, https://doi.org/10.1016/j.soilbio.2004.08.008, 2005.

Jones, D. L., Nguyen, C., and Finlay, R. D.: Carbon flow in the rhizosphere: Carbon trading at the soil-root interface. Plant and Soil, 321, 5–33, https://doi.org/10.1007/s11104-009-9925-0, 2009.

Klein, T., Siegwolf, R. T. W., and Körner, C.: Belowground carbon trade among tall trees in a temperate forest, Science, 352, 342–344, https://doi.org/10.1126/science.aad6188, 2016.

Koarashi, J., Hockaday, W. C., Masiello, C. A., and Trumbore, S. E, Dynamics of decadally cycling carbon in subsurface soils, J. Geophys. Res. Biogeos., 117, 1–13, https://doi.org/10.1029/2012JG002034, 2012.

Kruger, B. R., Werne, J. P., and Minor, E. C.: Sediment organic matter compositional changes in a tropical rift lake as a function of water depth and distance from shore. Org. Geochem., 175, 104527, https://doi.org/10.1016/j.orggeochem.2022.104527, 2023.

Kubota, K., Shirai, K., Murakami-Sugihara, N., Seike, K., Minami, M., Nakamura, T., and Tanabe, K. (2018). Bomb-^{14}C peak in the North Pacific recorded in long-lived bivalve shells (*Mercenaria stimpsoni*). J. Geophys. Res. Oceans, 123, 2867–2881, https://doi.org/10.1002/2017JC013678, 2018.

Kusch, S., Kashiyama, Y., Ogawa, N. O., Altabet, M., Butzin, M., Friedrich, J., Ohkouchi, N., and Mollenhauer, G.: Implications for chloro- and pheopigment synthesis and preservation from combined compound-specific $\delta^{13}C$, $\delta^{15}N$, and $\Delta^{14}C$ analysis. Biogeosciences, 7, 4105–4118, https://doi.org/10.5194/bg-7-4105-2010, 2010.

Formatted: Font: Italic

Landeweert, R., Hoffland, E., Finlay, R. D., Kuyper, T. W., and van Breemen, N.: Linking plants to rocks: ectomycorrhizal fungi mobilize nutrients from minerals. Trends Ecol. Evol., 16, 248–254, https://doi.org/10.1016/S0169-5347(01)02122-X, 2001.

Martin-Benito, D., Pederson, N., Férriz, M., and Gea-Izquierdo, G.: Old forests and old carbon: A case study on the stand dynamics and longevity of aboveground carbon. Sci. Total Environ., 765, 142737, https://doi.org/10.1016/j.scitotenv.2020.142737, 2021.

Masuda, T. and Fujita, Y.: Regulation and evolution of chlorophyll metabolism. Photochem. Photobiol. Sci., 7, 1131–1149, https://doi.org/10.1039/b807210h, 2008.

Matile, P., Stefan, H., and Thomas, H.: Chlorophyll degradation. Annu. Rev. Plant Physiol. Plant Mol. Biol., 50, 67–95, https://doi.org/10.1146/annurev.arplant.50.1.67, 1999.

Mészáros, I., Veres, S., Kanalas, P., Oláh, V., Szőllősi, E., Sárvári, É., Lévai, L., and Lakatos, G.: Leaf growth and photosynthetic performance of two co-existing oak species in contrasting growing seasons. Acta Silvatica et Lignaria Hungarica, 3, 7–20, https://doi.org/10.37045/aslh-2007-0001, 2007

Mollenhauer, G., Inthorn, M., Vogt, T., Zabel, M., Sinninghe Damsté, J. S., and Eglinton, T. I.: Aging of marine organic matter during cross-shelf lateral transport in the Benguela upwelling system revealed by compound-specific radiocarbon dating. Geochem. Geophys. Geosys., 8, Q09004, https://doi.org/10.1029/2007GC001603, 2007.

Moran-Zuloaga, D., Dippold, M., Glaser, B., and Kuzyakov, Y.: Organic nitrogen uptake by plants: reevaluation by position-specific labeling of amino acids: Reevaluation of organic N uptake by plants by position-specific labeling. Biogeochemistry, 125, 359–374, https://doi.org/10.1007/s10533-015-0130-3, 2015.

Muhr, J., Messier, C., Delagrange, S., Trumbore, S., Xu, X., and Hartmann, H.: How fresh is maple syrup? Sugar maple trees mobilize carbon stored several years previously during early springtime sap-ascent. New Phytol., 209, 1410–1416, https://doi.org/10.1111/nph.13782, 2016.

Näsholm, T., Ekblad, A., Nordin, A., Giesler, R., Högberg, M., and Högberg, P.: Boreal forest plants take up organic nitrogen. Nature, 392, 914–916, https://doi.org/10.1038/31921, 1998.

Oeschger, H., Siegenthaler, U., Schotterer, U., and Gugelmann, A.: A box diffusion model to study the carbon dioxide exchange in nature. Tellus A: Dynamic Meteorol. Oceanogr., 27, 168–192, https://doi.org/10.3402/tellusa.v27i2.9900, 1975.

Ogawa, N. O., Nagata, T., Kitazato, H., and Ohkouchi, N.: Ultra-sensitive elemental analyzer/isotope ratio mass spectrometer for stable nitrogen and carbon isotope analyses, in: Earth, Life, and Isotopes, edited by: Ohkouchi N., Tayasu I., and Koba, K., Kyoto University Press, Kyoto, Japan, 339–353, 2010.

Ohkouchi, N., Eglinton, T. I., Keigwin, L. D., and Hayes, J. M.: Spatial and temporal offsets between proxy records in a sediment drift, Science, 298, 1224–1227, https://doi.org/10.1126/science.1075287, 2002.

Randerson, J. T., Enting, I. G., Schuur, E. A. G., Caldeira, K., and Fung, I. Y.: Seasonal and latitudinal variability of troposphere $\Delta^{14}CO_2$: Post bomb contributions from fossil fuels, oceans, the stratosphere, and the terrestrial biosphere. Global Biogeochem. Cycles, 16, 59-1–59-19, https://doi.org/10.1029/2002gb001876, 2002.

Rasmussen, J., Sauheitl, L., Eriksen, J., and Kuzyakov, Y.: Plant uptake of dual-labeled organic N biased by inorganic C uptake: Results of a triple labeling study. Soil Biol. Biochem., 42, 524–527, https://doi.org/10.1016/j.soilbio.2009.11.032, 2010.

Reimer, P.J., Brown, T.A. and Reimer, R.W.: Discussion; reporting and calibration of post-bomb ^{14}C data. Radiocarbon 46, 1299–1304, https://doi.org/10.1017/S0033822200033154, 2004.

Richardson, A. D., Carbone, M. S., Huggett, B. A., Furze, M. E., Czimczik, C. I., Walker, J. C., Xu, X., Schaberg, P. G., and Murakami, P.: Distribution and mixing of old and new nonstructural carbon in two temperate trees. New Phytol., 206, 590–597, https://doi.org/10.1111/nph.13273, 2015.

Rodríguez-Calcerrada, J., Pardos, J. A., Gil, L., Reich, P. B., and Aranda, I.: Light response in seedlings of a temperate (*Quercus petraea*) and a sub-Mediterranean species (*Quercus pyrenaica*): Contrasting ecological strategies as potential keys to regeneration performance in mixed marginal populations, Plant Ecol., 195, 273–285, https://doi.org/10.1007/s11258-007-9329-2, 2008.

Simard, S. W., Perry, D. A., Jones, M. D., Myrold, D. D., Durall, D. M., and Molina, R.: Net transfer of carbon between ectomycorrhizal tree species in the field, Nature, 388, 579–582, https://doi.org/10.1038/41557, 1997.

Smith, S. E. and Read, D.: Structure and development of ectomycorrhizal roots, in: Mycorrhizal Symbiosis, 191–268, Academic Press, https://doi.org/10.1016/B978-012370526-6.50008-8, 2008.

Stuiver, M. and Polach, H. A.: Discussion reporting of ^{14}C data. Radiocarbon, 19, 355–363, https://doi.org/10.1017/S0033822200003672, 1977.

Suetsugu, K., Matsubayashi, J., and Tayasu, I.: Some mycoheterotrophic orchids depend on carbon from dead wood: novel evidence from a radiocarbon approach, New Phytol., 227, 1519–1529, https://doi.org/10.1111/nph.16409, 2020.

Taiz, L., Møller, I. M., Murphy, A., and Zeiger, E.: Plant Physiology and Development. Oxford University Press, https://doi.org/10.1093/hesc/9780197614204.001.0001, 2023.

Tayasu, I., Hirasawa, R., Ogawa, N. O., Ohkouchi, N., and Yamada, K.: New organic reference materials for carbon- and nitrogen-stable isotope ratio measurements provided by Center for Ecological Research, Kyoto University, and Institute of Biogeosciences, Japan Agency for Marine-Earth Science and Technology, Limnology, 12, 261–266, https://doi.org/10.1007/s10201-011-0345-5, 2011.

Trumbore, S.: Age of soil organic matter and soil respiration: Radiocarbon constraints on belowground C dynamics, Ecol. Appl., 10, 399–411, https://doi.org/10.1890/1051-0761(2000)010[0399:AOSOMA]2.0.CO;2, 2000.

van der Voort, T. S., Mannu, U., Hagedorn, F., McIntyre, C., Walthert, L., Schleppi, P., Haghipour, N., and Eglinton, T. I.: Dynamics of deep soil carbon – insights from ^{14}C time series across a climatic gradient, Biogeosciences, 16, 3233–3246, https://doi.org/10.5194/bg-16-3233-2019, 2019.

Vavilin, D. andVermaas, W.: Continuous chlorophyll degradation accompanied by chlorophyllide and phytol reutilization for chlorophyll synthesis in *Synechocystis* sp. PCC 6803. Biochim. Biophys. Acta Bioenergetics, 1767, 920–929, https://doi.org/10.1016/j.bbabio.2007.03.010, 2007.

Formatted: Superscript

Von Wettstein, D., Gough, S., and Kannangara, C. G.: Chlorophyll biosynthesis, Plant Cell, 7, 1039–1057, https://doi.org/10.2307/3870056, 1995.

Yamamoto, S., Miyairi, Y., Yokoyama, Y., Suga, H., Ogawa, N. O., and Ohkouchi, N.: Compound-specific radiocarbon analysis of organic compounds from Mount Fuji proximal lake (Lake Kawaguchi) sediment, central Japan, Radiocarbon, 62, 439–451, https://doi.org/10.1017/RDC.2019.158, 2020.

Page 5: [1] Formatted Table	Naoto Ishikawa	2/11/26 2:20:00 PM

Formatted Table

Page 5: [2] Formatted	Naoto Ishikawa	2/11/26 2:20:00 PM

Font: 8 pt

Page 5: [3] Formatted	Naoto Ishikawa	2/11/26 2:20:00 PM

Font: 8 pt

Page 5: [4] Formatted	Naoto Ishikawa	2/11/26 2:20:00 PM

Font: 8 pt

Page 5: [5] Formatted	Naoto Ishikawa	2/11/26 2:20:00 PM

Font: 8 pt

Page 5: [6] Formatted	Naoto Ishikawa	2/11/26 2:20:00 PM

Font: 8 pt

Page 5: [7] Formatted	Naoto Ishikawa	2/11/26 2:20:00 PM

Font: 8 pt

Page 5: [8] Formatted	Naoto Ishikawa	2/11/26 2:20:00 PM

Font: 8 pt

Page 5: [9] Formatted	Naoto Ishikawa	2/11/26 2:20:00 PM

Font: 8 pt

Page 5: [10] Formatted	Naoto Ishikawa	2/11/26 2:20:00 PM

Font: 8 pt

Page 5: [11] Formatted	Naoto Ishikawa	2/11/26 2:20:00 PM

Font: 8 pt

Page 5: [12] Formatted	Naoto Ishikawa	2/11/26 2:20:00 PM

Font: 8 pt

Page 5: [13] Formatted	Naoto Ishikawa	2/11/26 2:20:00 PM

Font: 8 pt

Page 5: [14] Formatted	Naoto Ishikawa	2/11/26 2:20:00 PM

Font: 8 pt

Page 5: [15] Formatted	Naoto Ishikawa	2/11/26 2:20:00 PM

Font: 8 pt

Page 5: [16] Formatted	**Naoto Ishikawa**	**2/11/26 2:20:00 PM**

Font: 8 pt

Page 5: [17] Formatted	**Naoto Ishikawa**	**2/11/26 2:20:00 PM**

Font: 8 pt

Page 5: [18] Formatted	**Naoto Ishikawa**	**2/11/26 2:20:00 PM**

Font: 8 pt

Page 5: [19] Formatted	**Naoto Ishikawa**	**2/11/26 2:20:00 PM**

Font: 8 pt

Page 5: [20] Formatted	**Naoto Ishikawa**	**2/11/26 2:12:00 PM**

Font: 8 pt

Page 5: [21] Formatted	**Naoto Ishikawa**	**2/11/26 2:12:00 PM**

Font: 8 pt

Page 5: [22] Formatted	**Naoto Ishikawa**	**2/11/26 2:12:00 PM**

Font: 8 pt

Page 5: [23] Formatted	**Naoto Ishikawa**	**2/11/26 2:12:00 PM**

Font: 8 pt

Page 5: [24] Formatted	**Naoto Ishikawa**	**2/11/26 2:12:00 PM**

Font: 8 pt

Page 5: [25] Formatted	**Naoto Ishikawa**	**2/11/26 2:12:00 PM**

Font: 8 pt

Page 5: [26] Formatted	**Naoto Ishikawa**	**2/11/26 2:12:00 PM**

Font: 8 pt

Page 5: [27] Formatted	**Naoto Ishikawa**	**2/11/26 2:12:00 PM**

Font: 8 pt

Page 5: [28] Formatted	**Naoto Ishikawa**	**2/11/26 2:12:00 PM**

Font: 8 pt

Page 5: [29] Formatted	**Naoto Ishikawa**	**2/11/26 2:21:00 PM**

Font: 8 pt

Page 5: [30] Formatted **Naoto Ishikawa** **2/11/26 2:21:00 PM**

Font: 8 pt

Page 5: [31] Formatted **Naoto Ishikawa** **2/11/26 2:21:00 PM**

Font: 8 pt

Page 5: [32] Formatted **Naoto Ishikawa** **2/11/26 2:21:00 PM**

Font: 8 pt

Page 5: [33] Formatted **Naoto Ishikawa** **2/11/26 2:21:00 PM**

Font: 8 pt

Page 5: [34] Formatted **Naoto Ishikawa** **2/11/26 2:21:00 PM**

Font: 8 pt

Page 5: [35] Formatted **Naoto Ishikawa** **2/11/26 2:21:00 PM**

Font: 8 pt

Page 5: [36] Formatted **Naoto Ishikawa** **2/11/26 2:21:00 PM**

Font: 8 pt

Page 5: [37] Formatted **Naoto Ishikawa** **2/11/26 2:21:00 PM**

Font: 8 pt

Page 5: [38] Formatted **Naoto Ishikawa** **2/11/26 2:21:00 PM**

Font: 8 pt

Page 5: [39] Formatted **Naoto Ishikawa** **2/11/26 2:21:00 PM**

Font: 8 pt

Page 5: [40] Formatted **Naoto Ishikawa** **2/11/26 2:21:00 PM**

Font: 8 pt

Page 5: [41] Formatted **Naoto Ishikawa** **2/11/26 2:21:00 PM**

Font: 8 pt

Page 5: [42] Formatted **Naoto Ishikawa** **2/11/26 2:21:00 PM**

Font: 8 pt

Page 5: [43] Formatted **Naoto Ishikawa** **2/11/26 2:21:00 PM**

Font: 8 pt

Page 5: [44] Formatted **Naoto Ishikawa** **2/11/26 2:21:00 PM**

Font: 8 pt

Page 5: [45] Formatted	**Naoto Ishikawa**	**2/11/26 2:21:00 PM**

Font: 8 pt

Page 5: [46] Formatted	**Naoto Ishikawa**	**2/11/26 2:21:00 PM**

Font: 8 pt

Page 5: [47] Formatted	**Naoto Ishikawa**	**2/11/26 2:30:00 PM**

Font: 8 pt

Page 5: [48] Formatted	**Naoto Ishikawa**	**2/11/26 2:30:00 PM**

Font: 8 pt

Page 5: [49] Formatted	**Naoto Ishikawa**	**2/11/26 2:30:00 PM**

Font: 8 pt

Page 5: [50] Formatted	**Naoto Ishikawa**	**2/11/26 2:30:00 PM**

Font: 8 pt

Page 5: [51] Formatted	**Naoto Ishikawa**	**2/11/26 2:30:00 PM**

Font: 8 pt

Page 5: [52] Formatted	**Naoto Ishikawa**	**2/11/26 2:30:00 PM**

Font: 8 pt

Page 5: [53] Formatted	**Naoto Ishikawa**	**2/11/26 2:30:00 PM**

Font: 8 pt

Page 5: [54] Formatted	**Naoto Ishikawa**	**2/11/26 2:30:00 PM**

Font: 8 pt

Page 5: [55] Formatted	**Naoto Ishikawa**	**2/11/26 2:30:00 PM**

Font: 8 pt

Page 5: [56] Formatted	**Naoto Ishikawa**	**2/11/26 2:30:00 PM**

Font: 8 pt

Page 5: [57] Formatted	**Naoto Ishikawa**	**2/11/26 2:30:00 PM**

Font: 8 pt

Page 5: [58] Formatted	**Naoto Ishikawa**	**2/11/26 2:30:00 PM**

Font: 8 pt

Page 5: [59] Formatted **Naoto Ishikawa** **2/11/26 2:30:00 PM**

Font: 8 pt

Page 5: [60] Formatted **Naoto Ishikawa** **2/11/26 2:30:00 PM**

Font: 8 pt

Page 5: [61] Formatted **Naoto Ishikawa** **2/11/26 2:30:00 PM**

Font: 8 pt

Page 5: [62] Formatted **Naoto Ishikawa** **2/11/26 2:30:00 PM**

Font: 8 pt

Page 5: [63] Formatted **Naoto Ishikawa** **2/11/26 2:30:00 PM**

Font: 8 pt

Page 5: [64] Formatted **Naoto Ishikawa** **2/11/26 2:30:00 PM**

Font: 8 pt

Page 5: [65] Formatted **Naoto Ishikawa** **2/11/26 2:30:00 PM**

Font: 8 pt

Page 5: [66] Formatted **Naoto Ishikawa** **2/11/26 2:30:00 PM**

Font: 8 pt

Page 5: [67] Formatted **Naoto Ishikawa** **2/11/26 2:30:00 PM**

Font: 8 pt